Chemical Engineering Journal 198–199 (2012) 219–227

Contents lists available at SciVerse ScienceDirect

Chemical Engineering Journal

journal homepage: www.elsevier.com/locate/cej

Modified mesoporous clay adsorbent for adsorption isotherm and kinetics of methylene blue

M. Auta, B.H. Hameed *

School of Chemical Engineering, Engineering Campus, Universiti Sains Malaysia, 14300 Nibong Tebal, Penang, Malaysia

HIGHLIGHTS

- Methylene blue was adsorbed on both raw and modified Ball clay.
- Modification of the clay was done by acid treatment, cation exchange and calcinations.
- The modification increased the surface area and pore volume of the clay.
- Modified Ball clay gave better adsorption capacity than the raw Ball clay.

ARTICLE INFO

Article history:
Received 9 March 2012
Received in revised form 21 May 2012
Accepted 22 May 2012
Available online 29 May 2012

Keywords:
Ball clay
Isotherm
Thermodynamics
Kinetics
Methylene blue

ABSTRACT

Adsorptive uptake of methylene blue (MB) by both raw and modified Ball clay (MBC) were investigated through batch adsorption experiment. Modification of the raw clay was done by acid treatment, cation exchange and calcination; the raw and modified clays were molded into beads and freeze dried. Brunauer Emmett Teller (BET), scanning electron microscopy (SEM), Energy-dispersive X-ray spectroscopy (EDX) and Fourier transformed infrared spectroscopy (FTIR) analysis were carried out on both clays. The mesoporous modified Ball clay (MBC) had percent increase of adsorption capacity and surface area of 188.60% and 820%, respectively than the raw Ball clay (RBC). Langmuir, Freundlich and Redlich–Peterson models were used to obtain isotherm parameters. Pseudo-second-order kinetic model described the adsorption processes which were more favorable at higher pH. Increase in temperature from 30 to 50 °C of MB adsorption on both RBC and MBC increased the degree of dispersion and the process was found to be physiosorptive, endothermic and spontaneous for MBC but non-spontaneous for RBC; this was obtained from the thermodynamic studies. The results showed that MBC can be used adequately to adsorb MB more efficiently than RBC.

1. Introduction

Most environmental problems have their solutions from the environment which are identified through research [1]. Clays are among the cheapest, abundant, environmentally friendly, ion exchangeable and non-toxic adsorbents that can be used to substitute the expensive commercial activated carbon in tackling environmental pollution problems [2,3]. They have found useful applications in adsorption process which is one of the simplest and effective methods with easy operational conditions for the treatment of aqueous textile effluents [4,5]. Some of the clays are either used in their natural state or beneficiated before usage through processes such as calcinations, acid activation, pillaring, anion and cation exchange, organic modification with polymers or molecules and so on [6].

Clays are composed of the octahedral (Al^{3+}, Fe^{2+}, Fe^{3+}, or Mg^{2+}) and tetrahedral (Si^{4+}) structures depending on the type of clay [7]. Pillaring or basal plane spacing (001) is carried out to expand the silica layer of clay through intercalation of cations from common sources such as hydroxyl aluminum, iron, titanium, gallium, chromium and zirconium. Pillaring of clays helps in transforming them into microporous and mesoporous materials and the pillars are stabilized through calcinations. The charge of the pillaring agent and cation exchange capacity (CEC) is considered to guarantee the stability of the pillared clay [8]. The resulting porosity adds value to the pristine clay and making them useful for environmental pollution control in relation to dyes adsorption, organic pollutants removal and so on [9]. Thermal analysis helps in comprehending variation in acidity and dehydroxylation calcination temperature of clays for high performance [10,11]. Acid treatment of clays aimed at increasing the surface area as well as the pore size is promoted through series of reactions. These includes reaction of the acid with different cations to form sulfates and chlorates that

* Corresponding author. Fax: +60 45941013.
E-mail address: chbassim@eng.usm.my (B.H. Hameed).

1385-8947/$ - see front matter © 2012 Elsevier B.V. All rights reserved.
http://dx.doi.org/10.1016/j.cej.2012.05.075

can easily be eliminated, leaching of the cations with hydrogen ions and substitution of exchangeable cations Ca^{2+}, Na^{+} or K^{+} with protons, Si^{4+} with Al^{3+}, and Al^{3+} with Mg^{2+} [12,13].

Aside kaoline and montmorrillonite which are the major classifications of clays, other sub types of clays exists which are identified according to their chemical composition in relation to the major classification [8]. Ball clay has over 70% of kaolin and composed of some little amount of quartz and other impurities [14]. It has been used to adsorb some heavy metal [15], and dyes [14], from aqueous solutions. Ball clay like other clays are negatively charged adsorbents often effective for binding of cationic dyes [16]. Several studies on methylene blue adsorption on clay have been extensively carried out. It has been used as a model for cationic dye effluent adsorption studies and for assessing the removal capacity of a specific adsorbent from aqueous phase; it has been one of the most recognized probe molecules often times when dealing with average pore size pollutant molecules greater or equal to 1.5 nm [17,18]. The abundance and low cost of this mineral resource Ball clay motivated the research of converting it to valuable adsorbent for the adsorption of methylene blue from waste water.

This study is aimed at beneficiating Ball clay, characterizing it for morphology, surface area, porosity, functional groups identification and testing adsorption capacity of both the modified and raw Ball clay as low cost adsorbents for Methylene blue (MB). It will encompass study of effect of initial MB concentration, effect of solution pH; thermodynamic, kinetic and isothermal studies of the adsorption process.

2. Materials and methods

2.1. Materials

The Ball clay was sourced locally from Malaysia. Analytical grade of Methylene blue (MB), aluminum hydroxide ($Al(OH)_3$) and sulfuric acid (H_2SO_4) were purchased from Sigma–Aldrich chemicals, R & M marketing Essex, UK and Merck chemical company, respectively; and used without further purification. The clay material was crushed, ground, sieved to a particle sizes of 20–45 μm and then dried in oven overnight at 100 °C. Chemical structure of the MB is shown in Scheme 1.

2.2. Preparation of clay adsorbents

The oven dried Ball clay was measured and mixed with sodium alginate to form paste that was transformed into beads; the beads were freeze dried and 1–2 mm sizes of the beads obtained were named raw Ball clay (RBC). The Ball clay was activated using 2 M H_2SO_4 solution through wet process at 90 °C for 3 h in a ratio of 0.2 g clay/mL (clay/acid). The clay was washed with distilled water to remove the excess acid. This was done until neutrality was attained in the activated clay solution. It was then dried in an oven for 6 h at 110 °C for further process. Thereafter, about 100 mL of 0.5 M $Al(OH)_3$ was prepared and added to the acid treated clay and refluxed for 2 h at 90 °C. The refluxed solution was allowed overnight before washing, after which it was dried in an oven at 110 °C and then calcined for 3 h at 500 °C. The calcined clay was made into paste using sodium alginate and the paste was transformed to beads (1–2 mm) and then freeze dried. The freeze dried clay were tagged modified Ball clay (MBC). Pictorial view of the RBC and MBC are shown in Fig. 1.

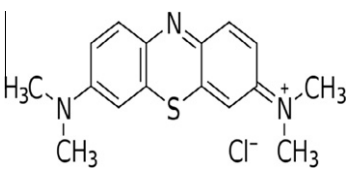

Scheme 1. Molecular structure of MB.

2.3. Characterization of the clay adsorbents

Elemental analysis, scanning electron microscopy (SEM) and surface area of the RBC and MBC were carried out using scanning electron microscope and Brunauer Emmett Teller (BET) analyzer, respectively.

Energy-dispersive X-ray spectroscopy (EDS or EDX) for elemental analysis and SEM were both carried out using scanning electron microscope (Model EMJEOL-JSM6301-F) with an Oxford INCA/ENERGY-350 microanalysis system.

The BET was carried out by nitrogen adsorption–desorption method using nitrogen temperature (−196 °C) with an autosorb BET apparatus, Micrometrics ASAP 2020, surface area and porosity analyzer. The analysis procedure was automated and operated with static volumetric techniques. The samples were first degassed at 200 °C for 2 h before each measurement was recorded.

Fourier transformed infrared spectroscopy (FTIR) analyses of MBC samples were performed using Perkin-Elmer Spectrum GX Infrared Spectrometer in the range of 4000–400 cm^{-1} with 4 cm^{-1} resolution. MBC sample and analytical grade KBr were dried at 100 °C over night and then ground together in a mixture ratio of 0.25 mg MBC to 100 mg of KBr. The mixture was used to produce disc which was used for FTIR analysis.

2.4. Batch equilibrium studies

An equilibrium adsorption study is an invaluable component of adsorption because it is the first requirement in the design of any adsorption process [19]. Batch equilibrium adsorption studies were carried out in a set of Erlenmeyer flasks (250 mL) with 200 mL of MB solutions at different initial concentration (30–300 mg/L) in them. About 0.2 g (1–2 mm) of RBC adsorbent was added, mixed and placed in water-bath isothermal shaker at 30 °C for 24 h, at 140 rpm shaker speed to attain equilibrium. Afterwards, temperature of water-bath shaker was adjusted to 40 °C and 50 °C, and similar procedure was repeated with another set of flasks containing same MB concentration. The final concentration of MB solution in the flasks after equilibrium was determined using UV–Vis spectrophotometer (Shimadzu UV/Vis 1601 spectrophotometer, Japan) at maximum wavelength of 668 for MB. The same procedure was repeated using MBC as adsorbent. The amount of the MB adsorbed

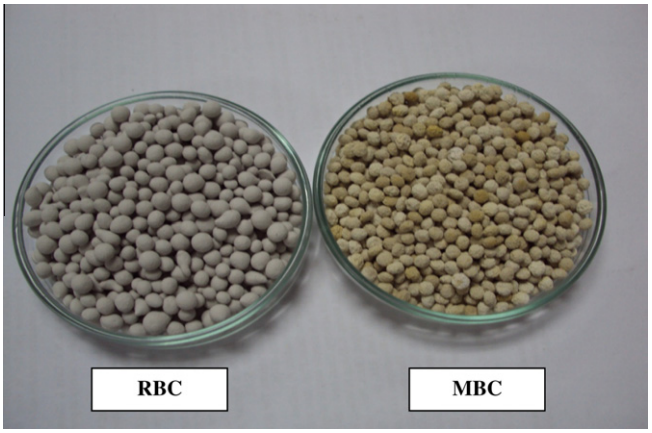

Fig. 1. Pictorial view of the MBC and RBC adsorbents.

at time t, at equilibrium Q_e (mg/g) was calculated using the following equation:

$$Q_e = \frac{(C_o - C_e)V}{W} \quad (1)$$

where C_o and C_e (mg/L) are the liquid-phase concentration of MB at initial and equilibrium, respectively; V (L) is the volume of the solution; and W (g) is the mass of the dry RBC or MBC adsorbent used.

2.5. Effect of solution pH

Effect of initial pH on the adsorption of MB on RBC and MBC was carried out by varying the initial pH of the solution from 3 to 12. The pH was adjusted using either 0.1 M HCl or 0.1 M NaOH solutions, and was measured using pH meter (Model Delta 320, Mettler Toledo, China). The study was conducted in a set of 250 mL Erlenmeyer flasks charged with 100 mg/L MB and 0.20 g of either RBC or MBC beads at a temperature of 30 °C for 24 h.

2.6. Batch kinetic studies

The study was conducted by determining the concentration of the MB solution at pre-set intervals of time. The amount of the dye adsorbed at time t, Q_t (mg/g) was calculated using equation:

$$Q_t = \frac{(C_o - C_t)V}{W} \quad (2)$$

where C_o and C_t (mg/L) are the liquid-phase concentration of the dye at the initial and any time t respectively; V (L) is the volume of the solution; and W (g) is the mass of the dried RBC or MBC adsorbent used.

2.7. Statistical analysis

Chi-square χ^2, statistical test is a ratio of sum of square difference between calculated data and experimental data to calculated data is expressed mathematically as:

$$\chi^2 = \frac{\sum(q_e - q_{e,m})^2}{q_{e,m}} \quad (3)$$

where q_e is the theoretical data and $q_{e,m}$ is the experimental data. The magnitude of χ^2 was used to determine the closeness of the calculated model data to the experimental data; the larger the χ^2 value, the higher the discrepancy between the data. Chi-square χ^2 test was used to determine the level of conformation of the calculated model values with the experimental values, a further check on the correlation coefficient R^2 results.

3. Results and discussion

3.1. Characterization of the adsorbents

Surface area and pore size of adsorbents are among important parameters that describe quality of adsorbents as they affect directly their analyte retention abilities. The RBC and MBC BET surface area, pore width and total pore volume obtained from the analysis were 10 m^2/g, 19.62 nm, 0.0519 cm^3/g and 92 m^2/g, 9.54 nm, 0.2183 cm^3/g, respectively. The RBC and MBC were mainly mesoporous in nature with physisorption isotherm of Type IV and H3 hysteresis loop features according to IUPAC classification [20]. Type IV physisorption isotherms are associated with capillary condensation taking place in mesopores, a limiting uptake over a range of high p/po and monolayer-multilayer adsorption features at the initial part of the isotherm. Similarly, TiO_2 mesoporous thin films studied by Atmospheric Ellipsometric Porosimetry reported type IV when mesoporosity measurement was carried out [21]. The isotherm plot showed that adsorption was not limited even at high p/po, an attribute of hysteresis H3. The BET surface area and sum of internal volume of pores in a gram of MBC, were higher than those of RBC. This may be attributed to leaching of some cations and loss of some sulfates compounds formed during the acid treatment and calcinations processes. The presence of these substances in the RBC were responsible for impeding diffusion of nitrogen into the core of the adsorbent during the BET analysis and eventually their removal after modification lead to recording of larger pore volume for nitrogen adsorption. Similar result has been reported when SP(0.0)-cal was treated ultrasonically and the treatment increased both surface area and pore volume of spheres [22]. The observed decrease of pore width after modification of the adsorbent was attributed to calcinations it was subjected to, which also resulted in the collapse of the pore structure. A similar report is found in literature stating the collapse of pore structure when porous titania was calcined at 550 °C [23]. The N_2 adsorption/desorption isotherms for the RBC and MBC are shown in Fig. 2.

The elemental analysis and morphological structure of RBC and MBC obtained are illustrated in Fig. 3. Depletion of some cations was observed in MBC signifying that leaching of such ions had occurred as well as loss of the affected ions in form of oxides and sulfate during calcinations; before modification we had 30.23 wt% of O, 2.51 wt% of Mg, 17.04 wt% of Al, 26.93 wt% of Si, 3.73 wt% of K, 0.72 wt% of Ca, 2.89 wt% of Ti, 15.96 wt% of Fe and after modification, we had 45.31 wt% of O, 0.00 wt% of Mg, 30.43 wt% of Al, 21.24 wt% of Si, 1.97 wt% of K, 0.50 wt% of Ca, 0.55 wt% of Fe. It has been reported that during acid treatment, some cations react with the acid to form sulfates, chlorates and oxides which can easily be loss from the adsorbent; also, leaching of some cations such as Na^+, K^+, Ca^{2+} occurs during acid treatment [24]. The morphological structure obtained revealed that the MBC particles were more clustered together in the RBC than the dispersed particles arrangement of the modified clay. The spaces between the dispersed MBC particles could be attributed to the loss of some volatile compounds. Similar observation was recorded for analysis of raw, pillared and calcined montmorillonite clay in a study for reactive adsorption of methylene blue via an ESI-MS [18].

The FTIR analysis was carried out to identify the functional groups present on the adsorbent and also study their effect on the adsorption. Points of symmetry on the spectra for MBC and modified Ball clay after adsorption (MBC-AA) were on wavenumbers

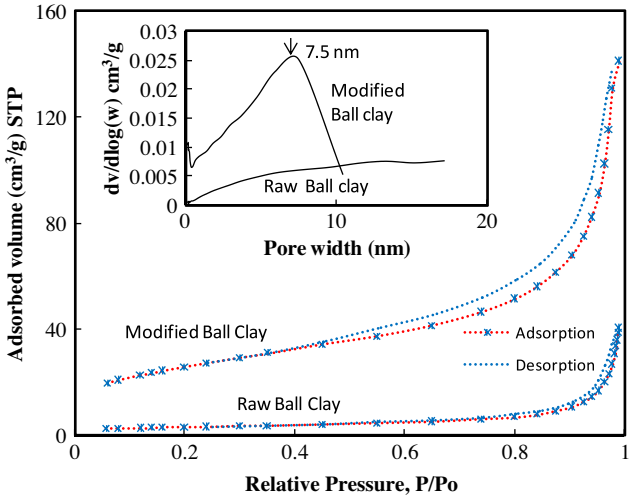

Fig. 2. The BET plot for raw and modified Ball clay.

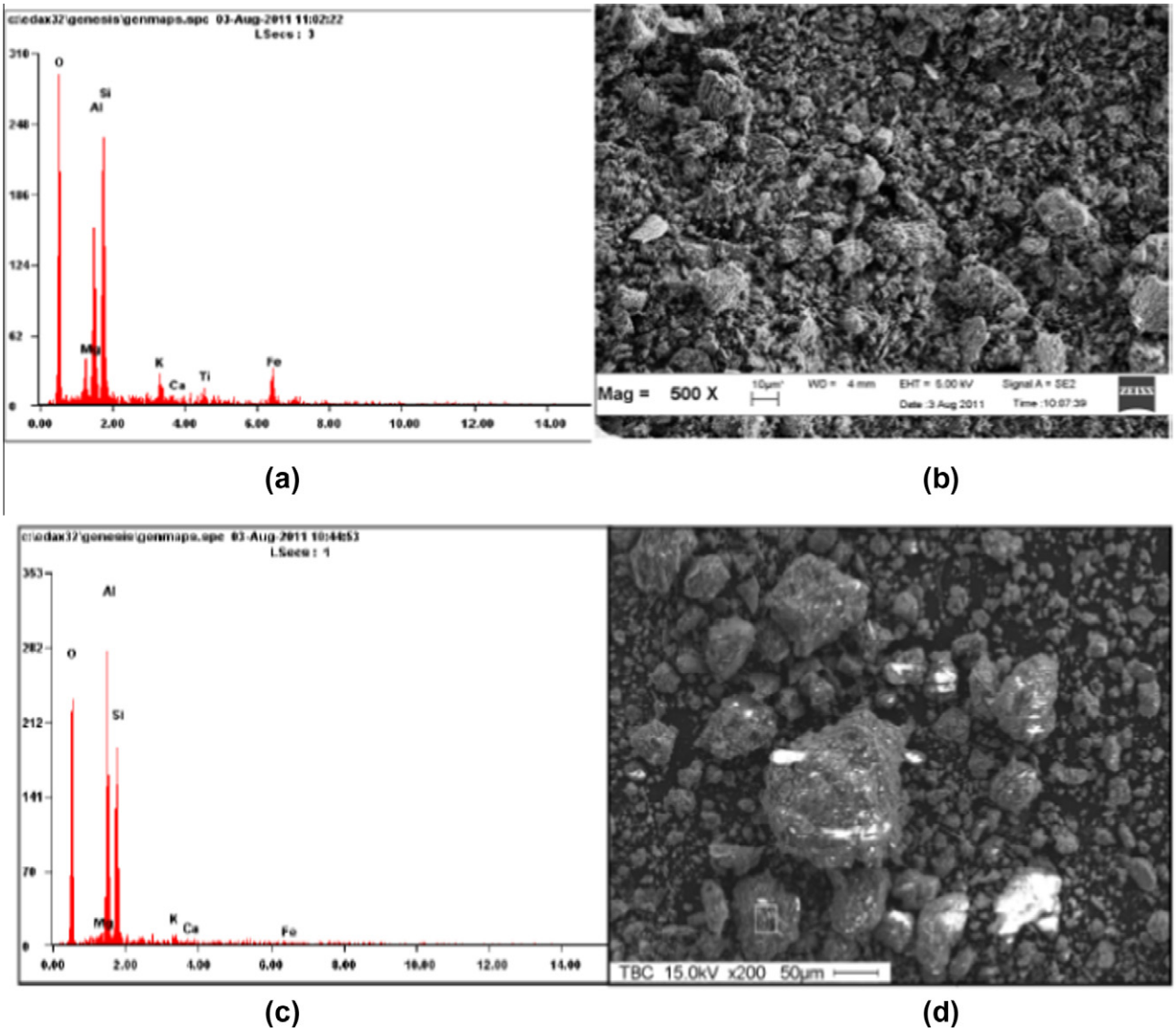

Fig. 3. The EDX and SEM analysis: (a) RBC spectrum, (b) RBC SEM, (c) MBC spectrum, (d) MBC SEM.

3429 and 1390 cm^{-1}, these points depicted –OH and NH_2 functional groups and NO_2 symmetric stretch of some Nitro functional groups, respectively. Some O–H stretching of silica group attributed to molecules coupling on surface of clays has been reported for Ball clay on similar wavenumbers [14]. In the course of the adsorption, some functional groups peaks became conspicuous which were not found in the MBC spectrum. These include S–O bends of inorganic sulfates at 617 cm^{-1} and scissors of NO_2 functional groups at 880 cm^{-1}. This was attributed to the MB molecule adsorbed on the MBC. Shifting and stretching of some functional groups peaks were noticed between the MBC and MBC-AA spectra. The CH, CH_2 and CH_3 functional groups located at wavenumbers 2957 cm^{-1} on MBC spectrum, shifted to 2927 cm^{-1} on MBC-AA spectrum. Similarly, saturated functional groups of carbon/hydrogen were also found on band width <3000 cm^{-1} [25,26]. The C=C benzene peak on 1570 cm^{-1} (MBC) shifted to 2927 cm^{-1} on MBC-AA spectrum at wavenumber 1554 cm^{-1}. There was no much difference in the Si—O—Si asymmetric stretch of silica between the spectra, but vibration in their wavenumbers was observed with 1045 and 1157 cm^{-1} on MBC and MBC-AA, respectively. Si—O—Si functional group on band width 1019 cm^{-1} due to effect of vibration elongation has been reported on Kaolin clay spectrum [27]. The numerous O—H and sulfonate functional groups on the surface of MBC may have contributed to adsorption of MB molecules. The FTIR of MBC and MBC-AA are shown in Fig. 4.

3.2. Effect of solution pH

Potency of hydrogen pH, of the MB solution was done to check favorability of ion-exchange process-common characteristics of MB adsorption on clay minerals [28]. The pH (3–12) studies results revealed that electrostatic and ion-exchange activities between the MB and adsorbent surface increased at elevated pH. The percentage removal of MB increased from 12% to 47% for RBC and 53% to 96% for MBC when the pH of the process was correspondingly increased from pH 3–12. It was attributed to presence of more negative charges adhering to positive charges of MB which resulted to high MB adsorption. Also, reduction of pH retarded the MB adsorption on both RBC and MBC which may be attributed to repulsion activities by similar ionic charges present that is the prevalence of H^+ in the acidic medium and cations of MB. Similar observations have been reported on MB adsorption on heat-treated palygorskite clay [29] and also on MB adsorption by activated carbon produced from steam activated bituminous coal [30]. The graph of effect of pH on MB adsorption by RBC and MBC is shown in Fig. 5.

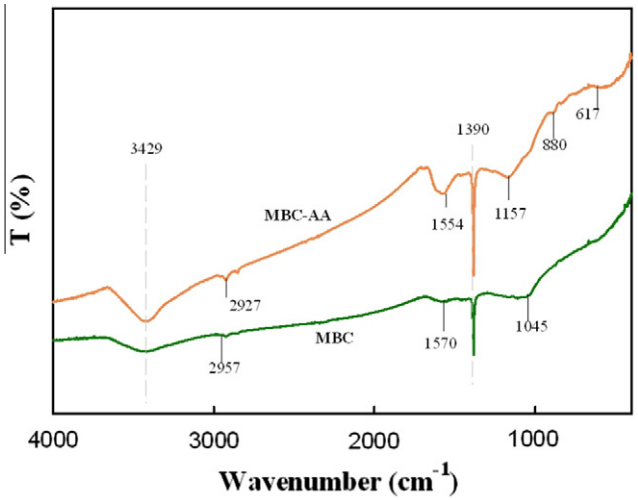

Fig. 4. The FTIR spectra of MBC and MBC-AA.

3.3. Effect of initial dye concentration and contact time on adsorption process

The effect of contact time on MB adsorption is shown in Fig. 6. The result obtained showed fast MB adsorption at initial stage with respect to the contact time and gradually became slower as equilibrium position was approached. Numerous and vacant active surface sites of the RBC and MBC were available at the initial stage of the reaction, and as the time lapsed, the vacant sites reduced in number thereby slowing down the adsorption process. Similarly, increase in initial MB concentration increased the loading rate of the adsorbate molecules for adsorption. It was attributed to increase in the driving force to the vacant active pores of the RBC and MBC [31]. But in terms of the percentage removal, the reverse was the case since at higher initial concentrations; outrageous MB molecules were in solution as compared with the available active vacant sites of the adsorbent. At lower initial MB concentration, the possibility of absolute uptake of limited MB molecules was higher leading to faster attainment of dynamic equilibrium; a condition where the amount of adsorbate in adsorbent was at equilibrium to the solute in the solution. The concentration adsorbed was determined with the aid of the UV–Vis spectrophotometer.

3.4. Effect of temperature on adsorption

The temperature variation from 30 to 50 °C on MB uptake by both RBC and MBC revealed that increase in temperature of the process enhanced better adsorption of MB from the bulk solution. Increase in temperature increased entropy of the system resulting to more successful collision of solute and adsorbent activities which yielded more chances of adsorption. The variation in adsorption at different temperatures was glaring from adsorptions capacities evaluated which are summarized in Table 1.

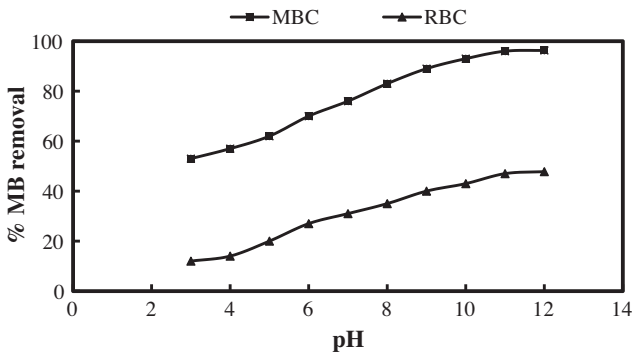

Fig. 5. Effect of pH of solution on MB adsorption by RBC and MBC (C_o = 100 mg/L, V = 200 mL, W = 0.20 g, shaking speed: 140 rpm, temperature = 30 °C).

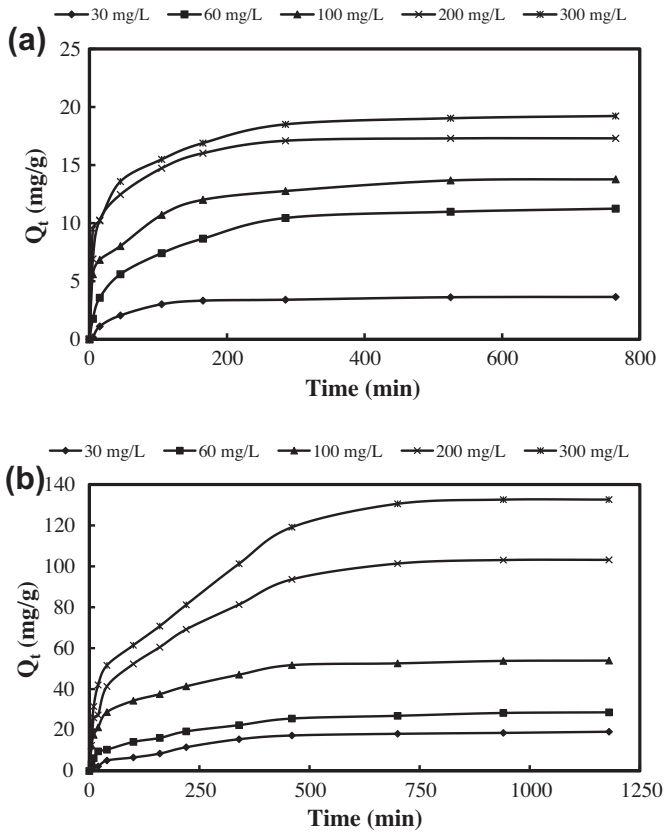

Fig. 6. Effect of initial MB concentration on (a) RBC adsorption and (b) MBC adsorption (V = 200 mL, W = 0.20 g, shaking speed = 140 rpm, temperature = 30 °C).

3.5. Adsorption isotherm studies for MB on RBC and MBC

The adsorbate distribution between the liquid phase and solid phase when the MB uptake had reached equilibrium was assessed by various adsorption isotherms. Three isotherm models namely: Langmuir, Freundlich and Redlich–Peterson were considered for the studies.

The non-linear form of the Langmuir isotherm model [32] is given as:

$$Q_e = \frac{Q_m C_e b}{1 + bC_e} \quad (4)$$

where C_e (mg/L), is the equilibrium concentration of MB adsorbed, Q_e (mg/g), is the amount of MB adsorbed, Q_m and b (Langmuir constants), the monolayer adsorption capacity and affinity of adsorbent towards adsorbate, respectively. Values of the Langmuir constants and profiles of sorption data are shown in Table 1 and Fig. 7, respectively.

Freundlich isotherm is based on the assumption that adsorption occurs on heterogenous surfaces with different energy of adsorption and non-identical rare sites. The non-linear form of the Freundlich model equation [33] used to investigate the MB adsorption process is given as:

$$Q_e = K_F C_e^{1/n} \quad (5)$$

Table 1
Langmuir, Freundlich and Redlich–Peterson parameters for MB adsorption on RBC and MBC at 30–50 °C.

Isotherms	Parameters	Raw Ball clay			Modified Ball clay		
		30 °C	40 °C	50 °C	30 °C	40 °C	50 °C
Langmuir	Q_m (mg/g)	25.010	30.179	34.652	62.500	66.670	100
	b (L/mg)	0.011	0.013	0.014	0.181	0.381	0.294
	R^2	0.982	0.980	0.974	0.913	0.898	0.902
	χ^2	6.603	2.553	3.262	1.846	4.656	5.612
Freundlich	K_F	1.530	2.099	2.475	3.155	15.031	14.256
	$1/n$	0.456	0.439	0.438	0.722	0.396	0.426
	R^2	0.994	0.982	0.987	0.924	0.915	0.905
	χ^2	5.983	0.499	1.552	1.193	2.314	4.413
Redlich–Peterson	g	0.693	0.616	0.595	0.374	0.224	0.046
	B (L/mg)	1.502	7.052	5.117	1.046	5.195	7.465
	A (L/g)	5.215	19.526	15.564	6.171	19.937	12.981
	R^2	1.000	0.983	0.990	0.973	0.917	0.912
	χ^2	0.669	0.175	0.101	1.000	0.897	0.122

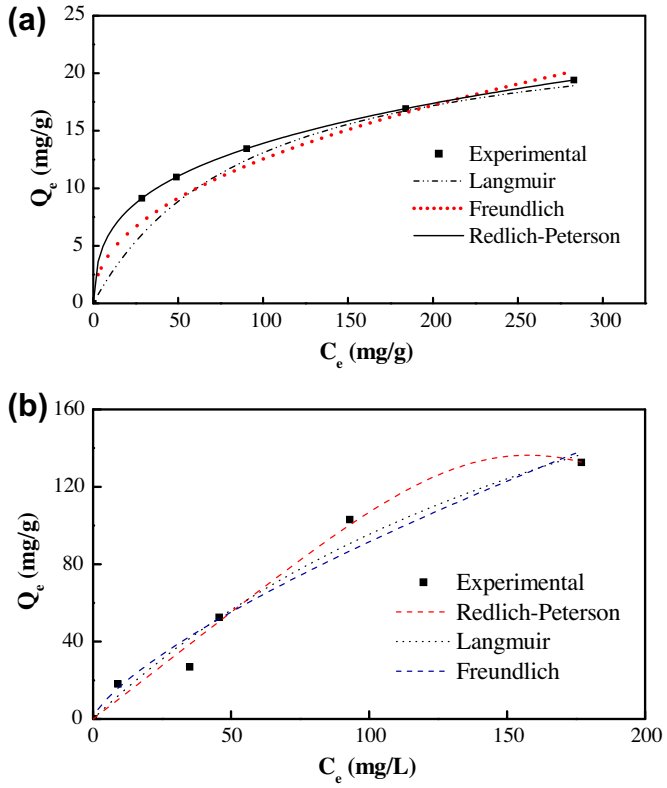

Fig. 7. Langmuir, Freundlich and Redlich–Peterson isotherms for MB adsorption on (a) RBC and (b) MBC at 30 °C.

where Q_e (mg/g) is the amount of dye adsorbed at equilibrium; C_e (mg/L) is the equilibrium concentration of the adsorbate; K_F and n are the Freundlich equilibrium constants. The heterogeneous factor n, gives information on favorability of adsorption process and $1/n$ values are related to the adsorption intensity; while K_F is the adsorption capacity of the adsorbate. Freundlich isotherm profile and parameters obtained are shown in Fig. 7 and Table 1, respectively.

The Redlich–Peterson isotherm model [34] contains three parameters and it involves features of both Langmuir and Freundlich isotherms. The equation is as follows:

$$Q_e = \frac{AC_e}{1 + BC_e^g} \tag{6}$$

Taking the natural logarithm gives the linear form of the equation as follows:

Table 2
Comparison of monolayer adsorption of MB onto various adsorbents.

Adsorbents	Maximum monolayer adsorption capacities (mg/g)	Refs.
Raw Ball clay	34.652	This work
Modified Ball clay	100	This work
SBA-15	51.176	[5]
Al-PILC	21	[9]
Zn-PILC	27	[9]
Montmorillonite	556	[18]
Pillard montmorillonite	81	[18]
Heated montmorillonite	62	[18]
Alkaline treated clinoptilolite	47.3	[1]

$$\ln\left(A\frac{C_e}{Q_e} - 1\right) = g\ln(C_e) + \ln(B) \tag{7}$$

The involvement of three parameters A, B, and g in the equation lead to development of a general trial and error procedure which is applicable to computer operations to determine the coefficient of determination, R^2 for series of values of A for the linear regression of $\ln(C_e)$ on $\ln[A(C_e/Q_e) - 1]$ and to obtain the best value of A which yields a maximum optimized value of R^2 was used [35]. The values of the Redlich–Peterson model parameters estimated and its profile are shown in Table 1 and Fig. 7, respectively.

Langmuir isotherm model evaluation in this study showed that the adsorption process was described by monolayer coverage of MB over both the RBC and MBC surfaces although there was low affinity on interaction between the adsorbate- adsorbent [36]; this was revealed by the low values of their correlation coefficients R^2. Modification carried out on the Ball clay lead to development of internal volume of the adsorbent as seen in the specific pore volume values which increased to 0.2183 cm^3/g from 0.0519 cm^3/g. The ability of this larger pore volume to retain more of the MB molecules was manifested in the higher adsorption capacity of MBC (100 mg/g) as compared with that of RBC (34.652 mg/g). The adsorption capacities obtained in this study are comparable with other adsorbents adsorption capacities of MB as shown in Table 2. The nature of the Freundlich model parameters K_F, n and $1/n$ obtained as seen in Table 1, showed that the adsorption process was favorable ($n > 1$) and there was high possibility of multilayer adsorption of MB through percolation process on the active heterogeneous surface ($0 < 1/n < 1$) sites of both RBC and MBC. The active energetic heterogeneity of MBC may be due to its irregular

Table 3
Pseudo-first and pseudo-second-order models parameters for MB adsorption on RBC and MBC at 30 °C.

Clay	Dye conc. (mg/L)	$Q_{exp.}$ (mg/g)	Pseudo-first-order parameters			Pseudo-second-order parameters		
			k_1 (h^{-1})	Q_{cal}	R^2	k_2 (10^4)	Q_{cal}	R^2
RBC	30	3.620	0.020	3.532	0.992	65.900	3.926	0.991
	60	10.981	0.014	10.629	0.952	18.000	11.754	0.984
	100	13.477	0.048	12.256	0.837	55.300	13.118	0.926
	200	17.296	0.073	15.992	0.921	59.900	17.021	0.978
	300	19.031	0.082	17.176	0.854	65.300	18.207	0.934
MBC	30	18.154	0.004	19.156	0.985	2.070	23.248	0.983
	60	26.944	0.007	26.910	0.912	3.770	29.690	0.952
	100	52.567	0.023	47.837	0.874	5.830	52.407	0.950
	200	103.079	0.007	98.360	0.917	1.030	108.575	0.955
	300	132.599	0.006	128.151	0.887	0.666	141.457	0.925

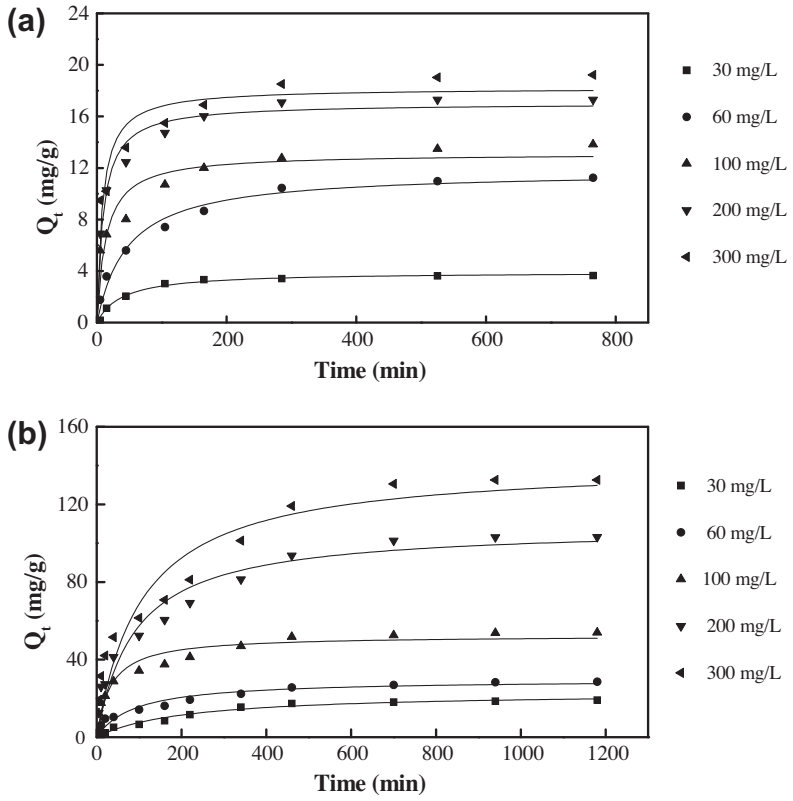

Fig. 8. Pseudo-second-order kinetic model plot for MB adsorption on (a) RBC and (b) MBC (V = 200 mL, W = 0.20 g, shaking speed = 140 rpm, temperature = 30 °C).

pore shape, pore size, surface functional groups and the presence of impurities [37]. The relatively high correlation coefficient R^2 value of Freundlich model further depicted the assertion that Freundlich adsorption isotherm gives an excellent representation of data for moderate partial pressures and concentrations but performs poorly with dilute concentrations [34]. The Redlich–Peterson isotherm parameter's values g determined revealed that the model was tending towards Freundlich and not Langmuir. This was because the g values obtained were far from unity as opposed to Langmuir model which is satisfied when the Redlich–Peterson g = 1. This further revealed that the adsorption of MB on MBC was not by monolayer arrangement, but by ion-exchange and complexation interactions as a result of full coverage of surface functional groups of the adsorbent via surface exchange reactions [3]. The order of fitness models from the best to the least was Redlich–Peterson, Freundlich and Langmuir isotherms based on their R^2 values; this is similar to methods of evaluation reported [38,39]. Also, in the study carried out to determine the regression analysis for the sorption isotherms of basic dyes on sugarcane dust, a similar trend of sequence as obtained in this study was the order reported [35].

The assertion that sometimes correlation coefficient, R^2 does not justify basis for selection of best fit of adsorption model [40], was investigated by use of Chi-square χ^2 statistical test. Chi-square χ^2 test was the best method of error fitting for adsorption of Congo red on palm kernel seed coat and lead on kernel fiber [41,42]. Using Chi-square error test, it has been reported in a study of Cr (VI) removal from Aqua system that Temkin isotherm model which had lowest R^2 than Langmuir and Freundlich models, showed more conformity of predicted values to the experimental values [43]. However, the χ^2 test results obtained in this study further supported that Redlich–Peterson was the best model that described the process of adsorption of MB on both RBC and MBC as revealed by correlation coefficient exitus. This was revealed by smaller values of χ^2 signifying stronger alliance between theoretical and experiment data as compare with Freundlich and Langmuir models. At temperatures of 30 and 50 °C for RBC and MBC respectively,

both Freundlich and Langmuir models' data conformity with the theoretical data were similar, as seen by smaller variations in the magnitude of their χ^2 values.

3.6. Adsorption kinetic models

3.6.1. Pseudo-first order model

The non-linear pseudo-first order equation [44] is given as:

$$Q_t = Q_e(1 - e^{k_1 t}) \quad (8)$$

where Q_e and Q_t (mg/g), are the amount of MB dye adsorbed at equilibrium and at time t (h) respectively; k_1 (h^{-1}), is the rate constant of adsorption. Plots of Q_t against t, at various temperatures studied were plotted (figures not shown) for the two adsorbents and the parameters obtained are presented in Table 3.

3.6.2. Pseudo-second order model

The pseudo-second order equilibrium adsorption model [45] equation is given as:

$$Q_t = \frac{k_2 Q_e^2 t}{(1 + k_2 Q_e t)} \quad (9)$$

where k_2 (g/mgh) is the rate constant of second order adsorption. The Fig. 8 represents plots of Q_t versus t at 30 °C which gave very good curves. The model's parameters generated from the plots for adsorption of MB on RBC and MBC are presented in Table 3.

When the initial MB concentration was 30 mg/L, its adsorption on the two adsorbents RBC and MBC was found to fit very well the pseudo-first-order kinetics as shown by the values of correlation coefficient R^2 which were the highest. But on the whole, the assertion that Lagergren model does not fit well in an entire contact time but mostly suitable over the initial stage of the adsorption process was glaring [46]. This was revealed by the low R^2 values obtained as compared with those of pseudo-second-order model's values. The MB adsorption mechanism on either RBC or MBC was the rate controlling step going by the good correlation between the calculated and experimental data of the entire range of adsorption behavior explained by pseudo-second-order kinetic model. This shows that pseudo-second-order model with the least R^2 values of 0.926 for RBC and 0.925 MBC were more applicable for description of the whole MB adsorption as compared with their pseudo-first-order model least R^2 values of 0.837 and 0.874, respectively. This observation is consistent with similar phenomenon on sorption of MB reported [47,48].

3.7. Adsorption thermodynamics

Thermodynamic studies are useful for interpretation of adsorption behaviors especially as it concerns equilibrium of the process [49]. Adsorption of MB on both RBC and MBC thermodynamic studies were carried out at various temperatures of 30, 40 and 50 °C. The Gibb's free energy of the process was determined using the following equation:

$$\Delta G = RT \ln K_o \quad (10)$$

where R is the universal gas constant (8.314 J/K mol); T (K) the absolute temperature; K_o is the distribution coefficient expressed as $K_o = Q_e/C_e$; and, ΔG is the Gibbs free energy.

The average standard enthalpy change of MB adsorption on RBC and MBC were determined using Van't Hoff equation which is expressed as:

$$\ln K_o = \frac{\Delta G}{RT} = \frac{\Delta S}{R} - \frac{\Delta H}{RT} \quad (11)$$

The values of ΔS and ΔH were obtained from intercept and slope, respectively of plot of InKo against $1/T$ (figure not shown).

Table 4
Thermodynamics parameters for MB adsorption on RBC and MBC.

Clay	ΔH (kJ/mol)	ΔS (kJ/mol)	ΔG (kJ/mol)		
			303 K	313 K	323 K
RBC	47.831	0.141	5.209	3.289	2.462
MBC	76.115	0.260	−1.765	−6.941	−6.799

The absolute value of change of Gibbs free energy for physical adsorption is −20 to 0 kJ/mol which is smaller than that of chemisorptions −80 to −400 kJ/mol [50,51]. Negative values of Gibbs free energy obtained as seen in Table 4, show that the MB adsorption on MBC was spontaneous and physical in nature; but MB adsorption on RBC was non-spontaneous which was revealed by the positive values of ΔG at all temperatures under study. A non-spontaneous adsorption of Cr(III) on activated carbon has been reported at all temperatures under investigation [52]. The results also showed that both enthalpy and entropy's values were positive signifying that the adsorption process was endothermic and the degree of dispersion increased with increase in temperature. The endothermic behavior observed from enthalpy values further confirmed the trend of adsorption of MB on the adsorbents which were found to increase as the temperature was increased. This is in line with report on the study of adsorption of Rhodamine B unto low cost adsorbents [53].

4. Conclusion

This study revealed that modification of the mesoporous Ball clay lead to development of large surface area and pore volume, this was revealed by the characterization analysis of the adsorbents. The MBC was found to be a better and more effective adsorbent than RBC that can be used to remove MB from aqueous solution. The adsorption processes for the two adsorbents were found to be dependent on the solution pH, initial concentration of MB and solution temperature. Redlich–Peterson, Freundlich and Langmuir models in downward manner, was the order of fitness of the isotherms to the adsorption process for the adsorbents which both followed pseudo-second-order kinetic model. Thermodynamic studies revealed that physisorption was the nature of MB adsorption on both RBC and MBC which were also found to be endothermic and the degree of dispersion increased with increase in temperature. The MB adsorption on RBC was non-spontaneous while it was spontaneous on MBC.

References

[1] M. Akgul, A. Karabakan, Promoted dye adsorption performance over desilicated natural zeolite, Micropor. Mesopor. Mater. 145 (2011) 157–164.
[2] C. Bertagnolli, S.J. Kleinübing, M.G. Carlos da Silva, Preparation and characterization of a Brazilian bentonite clay for removal of copper in porous beds, Appl. Clay Sci. 53 (2011) 73–79.
[3] M. Toor, B. Jin, Adsorption characteristics, isotherm, kinetics, and diffusion of modified natural bentonite for removing diazo dye, Chem. Eng. J. 187 (2012) 79–88.
[4] A. Xue, S. Zhou, Y. Zhao, X. Lu, P. Han, Adsorption of reactive dyes from aqueous solution by silylated palygorskite, Appl. Clay Sci. 48 (2010) 638–640.
[5] V. Vimonsesa, B. Jina, C.W.K. Chow, C. Saint, Development of a pilot fluidised bed reactor system with a formulated clay–lime mixture for continuous removal of chemical pollutants from wastewater, Chem. Eng. J. 158 (2010) 535–541.
[6] B. Cheknane, O. Bouras, M. Baudu, J.P. Basly, A. Cherguielaine, Granular inorgano–organo pillared clays (GIOCs): preparation by wet granulation, characterization and application to the removal of a basic dye (BY28) from aqueous solutions, Chem. Eng. J. 158 (2010) 528–534.
[7] P. Liu, L. Zhang, Adsorption of dyes from aqueous solutions or suspensions with clay nano-adsorbents, Sep. Purif. Technol. 58 (2007) 32–39.
[8] J.-Q. Jiang, S.M. Ashekuzzaman, Development of novel inorganic adsorbent for water treatment, Curr. Opin. Chem. Eng. (2012), http://dx.doi.org/10.1016/j.coche.2012.03.008.

[9] A. Gil, F.C.C. Assis, S. Albeniz, S.A. Korili, Removal of dyes from wastewaters by adsorption on pillared clays, Chem. Eng. J. 168 (2011) 1032–1040.
[10] P. Li, Siddaramaiah, N.H. Kim, S. Heo, J. Lee, Novel PAAm/Laponite clay nanocomposite hydrogels with improved cationic dye adsorption behavior, Composites: Part B 39 (2008) 756–763.
[11] G.K. Sarma, S.S. Gupta, K.G. Bhattacharyya, Adsorption on natural and modified clays, separation science and technology, Sep. Sci. Technol. 46 (2011) 1602–1614.
[12] P. Kumar, R.V. Jasra, T.S.G. Bhat, Evolution of porosity and surface acidity in montmorillonite clay on acid activation, Ind. Eng. Chem. Res. 34 (1995) 1440–1448.
[13] J. Temuujin, M. Senna, T. Jadambaa, D. Burmaa, S. Erdenechimeg, K.J.D. MacKenzie, Characterization and bleaching properties of acid-leached montmorillonite, J. Chem. Technol. Biotechnol. 81 (2006) 688–693.
[14] P. Monash, R. Niwas, G. Pugazhenthi, Utilization of Ball clay adsorbents for the removal of crystal violet dye from aqueous solution, Clean Technol. Environ. Policy 13 (2011) 141–151.
[15] V. Chantawong, N.W. Harvey, V.N. Bashkin, Comparison of heavy metal adsorptions by Thai kaolin and Ballclay, Water Air Soil Pollut. 148 (2003) 111–125.
[16] M. Roulia, A.A. Vassiliadis, Sorption characterization of a cationic dye retained by clays and perlite, Micropor. Mesopor. Mater. 116 (2008) 732–740.
[17] B.S. Girgis, A.N.A. El-Hendawy, Porosity development in activated carbons obtained from date pits under chemical activation with phosphoric acid, Micropor. Mesopor. Mater. 52 (2002) 105–117.
[18] F.G.E. Nogueira, J.H. Lopes, A.C. Silva, M. Gonçalves, A.S. Anastácio, K. Sapag, L.C.A. Oliveira, Reactive adsorption of methylene blue on montmorillonite via an ESI-MS study, Appl. Clay Sci. 43 (2009) 190–195.
[19] M.G. Plaza, A.F.P. Ferreira, J.C. Santos, A.M. Ribeiro, U. Müller, N. Trukhan, J.M. Loureiro, A.E. Rodrigues, Propane/propylene separation by adsorption using shaped copper trimesate MOF, Micropor. Mesopor. Mater. (2011), http://dx.doi.org/10.1016/j.micromeso.2011.06.024.
[20] K.S.W. Sing, D.H. Everett, R.A.W. Haul, L. Moscou, R.A. Pierotti, J. Rouquerol, T. Siemieniewska, Reporting physisorption data for gas/solid systems with special reference to the determination of surface area and porosity, Pure Appl. Chem. 57 (1985) 603–619.
[21] O. Dubreuil, J. Dewalqu, G. Chene, F. Mathis, G. Spronck, D. Strivay, R. Cloots, C. Henrist, Tio_2 mesoporous thin films studied by atmospheric ellipsometric porosimetry: a case of contamination, Micropor. Mesopor. Mater. 145 (2011) 1–8.
[22] T. Watanabe, Y. Miki, T. Masuda, H. Kanai, S. Hosokawa, K. Wada, M. Inoue, Pore structure of γ-Ga_2O_3–Al_2O_3 particles prepared by spray pyrolysis, Micropor. Mesopor. Mater. 145 (2011) 131–140.
[23] C. Tian, Y. Yang, H. Pu, Effect of calcinations temperature on porous titania prepared from industrial titanyl sulfate solution, Appl. Surf. Sci. 257 (2011) 8391–8395.
[24] Z.B. Molu, K. Yurdakoc, Preparation and characterization of aluminum pillared K10 and KSF for adsorption of trimethoprim, Micropor. Mesopor. Mater. 127 (2010) 50–60.
[25] M. Auta, B.H. Hameed, Preparation of waste tea activated carbon using potassium acetate as an activating agent for adsorption of Acid Blue 25 dye, Chem. Eng. J. 171 (2011) 502–509.
[26] B.H. Hameed, M.I. El-Khaiary, Removal of basic dye from aqueous medium using a novel agricultural waste material: pumpkin seed hull, J. Hazard. Mater. 155 (2008) 601–609.
[27] K.L. Konan, C. Peyratout, A. Smith, J.-P. Bonnet, S. Rossignol, S. Oyetola, Comparison of surface properties between kaolin and metakaolin in concentrated lime solutions, J. Colloid Interf. Sci. 339 (2009) 103–109.
[28] D. Ghosh, K.G. Bhattacharyya, Adsorption of methylene blue on kaolinite, Appl. Clay Sci. 20 (2002) 295–300.
[29] H. Chen, J. Zhao, A. Zhong, Y. Jin, Removal capacity and adsorption mechanism of heat-treated palygorskite clay for methylene blue, Chem. Eng. J. 174 (2011) 143–150.
[30] E.N. El Qada, S.J. Allen, G.M. Walker, Adsorption of methylene blue onto activated carbon produced from steam activated bituminous coal: a study of equilibrium adsorption isotherm, Chem. Eng. J. 124 (2006) 103–110.
[31] I.A.W. Tan, A.L. Ahmad, B.H. Hameed, Adsorption of basic dye using activated carbon prepared from oil palm shell: batch and fixed bed studies, Desalination 225 (2008) 13–28.
[32] I. Langmuir, The constitution and fundamental properties of solids and liquids, J. Am. Chem. Soc. 38 (1916) 2221–2295.
[33] H.M.F. Freundlich, Over the adsorption in solution, J. Phys. Chem. 57 (1906) 385–470.
[34] O. Redlich, D.L. Peterson, A useful adsorption isotherm, J. Phy. Chem. 63 (1959) 1024.
[35] Y. Ho, W. Chiu, C. Wang, Regression analysis for the sorption isotherms of basic dyes on sugarcane dust, Bioresour. Technol. 96 (2005) 1285–1291.
[36] B.H. Hameed, H. Hakimi, Utilization of durian (*Durio zibethinus* Murray) peel as low cost sorbent for the removal of acid dye from aqueous solutions, Biochem. Eng. J. 39 (2008) 338–343.
[37] M.S. Balathanigaimani, W. Shim, K.H. Park, J. Lee, H. Moon, Effects of structural and surface energetic heterogeneity properties of novel corn grain-based activated carbons on dye adsorption, Micropor. Mesopor. Mater. 118 (2009) 232–238.
[38] A. Dheetcha, S. Mishra, Biosequestering potential of spirulina platensis for uranium, Curr. Microbio. 57 (2008) 508–514.
[39] J. Yang, K. Qiu, Preparation of activated carbons from walnut shells via vacuum chemical activation and their application for methylene blue removal, Chem. Eng. J. 165 (2010) 209–217.
[40] S. Azizian, B. Yahyaei, Adsorption of 18-crown-6 from aqueous solution on granular activated carbon: a kinetic modeling study, J. Colloid Interf. Sci. 299 (2006) 112–115.
[41] N.A. Oladoja, K.A. Akinlabi, Congo red biosorption on palm kernel seed coat, Ind. Eng. Chem. Res. 48 (2009) 6188–6196.
[42] Y.S. Ho, T.H. Chiang, Y.M. Hsueh, Proc. Biochem. 40 (2005) 119.
[43] N.A. Oladoja, I.A. Ololade, S.E. Olaseni, V.O. Olatujoye, O.S. Jegede, A.O. Agunloye, Synthesis of nano calcium oxide from a gastropod shell and the performance evaluation for Cr (VI) removal from aqua system, Ind. Eng. Chem. Res. 51 (2012) 639–648.
[44] S. Lagergren, B.K. Svenska, On the theory of so-called adsorption of dissolved substances, The Royal Swedish Academy of Sciences Document, Band 24 (1898) 1–13.
[45] Y.S. Ho, S. McKay, Pseudo-second order model for sorption processes, Process Biochem. 34 (1999) 451–465.
[46] Y.S. Ho, G. McKay, The sorption of lead (II) ions on peat, Water Res. 33 (1999) 578–584.
[47] B.H. Hameed, Evaluation of papaya seeds as a novel non-conventional low-cost adsorbent for removal of methylene blue, J. Hazard. Mater. 162 (2009) 939–944.
[48] N. Nasuha, B.H. Hameed, T. Azam, Mohd Din, Rejected tea as a potential low-cost adsorbent for the removal of methylene blue, J. Hazard. Mater. 175 (2010) 126–132.
[49] F.N. Ridha, P.A. Webley, Entropic effects and isosteric heats of nitrogen and carbon dioxide adsorption on chabazite zeolites, Micropor. Mesopor. Mater. 132 (2010) 22–30.
[50] M.J. Jaycock, G.D. Parfitt, Chemistry of Interfaces, Ellis Horwood, Onichester, 1981. pp. 12–13.
[51] Q. Li, Q. Yue, Y. Su, B. Gao, H. Sun, Equilibrium, thermodynamics and process design to minimize adsorbent amount for the adsorption of acid dyes onto cationic polymer-loaded bentonite, Chem. Eng. J. 158 (2010) 489–497.
[52] R.M. Schneider, C.F. Cavalin, M.A.S.D. Barros, C.R.G. Tavares, Adsorption of chromium ions in activated carbon, Chem. Eng. J. 132 (2007) 355–362.
[53] L. Li, S. Liu, T. Zhu, Application of activated carbon derived from scrap tires for adsorption of Rhodamine B, J. Environ. Sci. 22 (2010) 1273–1280.